Special Brief Papers

Image-Motion Detection Using Analog VLSI

Chu Phoon Chong, C. Andre T. Salama, and Kenneth C. Smith

Abstract—**Motion detection by differentiating the output currents of photosensors arranged in a 2D array is described. Subnanoampere current differentiation is made possible by the use of a novel current-mirror (CM) differentiator that requires only four MOSFET's. The pixel density of the motion-detecting imager is higher than 40 pixels/mm^2. Experimental results of the CM differentiator are reported.**

I. Introduction

In real-time image processing, the impracticality of integrating an A/D converter and a simple processor with each pixel in an imager requires the sequential digitization of the signals generated by the pixels. While parallel execution of different parts of the algorithm can be done using multiple processors, the sequential nature of data input will limit the degree of parallel processing of the digital system to a level lower than that achievable by image processing systems with parallel data generation and input. Currently, image processing systems with parallel data generation and processing are almost exclusively analog. Only an analog processor that occupies a much smaller area than its digital counterpart and does not require A/D conversion can be integrated with each pixel in an imager without leading to impractically low pixel density.

Finding alternative analog processing arrays that do not require A/D conversion has attracted considerable attention [1]–[3]. While some of these analog processing arrays are inspired directly by their biological counterparts [4], the others are analog implementations of known algorithms that do not resemble any processing technique used in biological neural systems [5]. In this brief paper, the focus is on image-motion detection using analog VLSI techniques.

II. The Need for Motion Detection

In nature, an animal cannot stay in a highly alert state in order to guard itself against predators without fatigue and eventual breakdown of its nervous system. In the visual neural networks of most animals, there are numerous motion-detecting neurons. These neurons, whenever triggered by the movement of an approaching object, will send an alerting signal to the central nervous system. In this way, the animal, which may be in a relaxed state, is excited into a state of alertness. The incorporation of the motion-detection[1] capability into an artificial vision system can significantly reduce the amount of stored or transmitted redundant information by identifying and eliminating repetitive frames.

III. System Architecture

If the intensity of the image is time invariant and is only spatially variant, real-time image-motion detection can be performed using temporal differentiation of the output current of the photosensor.[2] When a time-invariant spatially variant image is projected onto an array of photodiodes, the intensity of the light falling onto a photodiode, and thus its output current, is constant over time. When a temporal differentiator is used to differentiate the output of the photodiode, the output of the differentiator is zero if the image is stationary. When the image moves, the spatially varying light intensity of the image will cause step changes in the output current of the photodiodes. Thus, the temporal differentiator will produce a nonzero output voltage (or current) proportional to the first derivative of the output current of the photodiode.

The system architecture of the imager is shown in Fig. 1. Using a voltage-to-current converter the output voltage of the current differentiator is converted to an output current of the pixel (consisting of the photodiode, the current differentiator, and the V–I converter). The output current of each pixel is sampled through two switches connected in series. One switch is controlled by the signal generated by the y-shift register and the other is controlled by the signal generated by the x-shift register. The local sampling architecture shown in Fig. 1 is used for experimental characterization of the imager only. In actual applications, the output current of all pixels is summed up to produce a wired-OR logic function. A load resistance R is used as the pull-up resistor for the wired-OR logic gate. Whenever the image moves, the wired-OR logic gate produces an asserted low global interrupt signal for an external controller and A/D converter to start the process of image digitization and transmission. However, observing the output of the wired-OR logic gate externally will not

Manuscript received May 14, 1991; revised September 5, 1991. This work was supported by the Natural Science and Engineering Research Council of Canada, the Canadian Microelectronics Corporation, ITRC, and MicroNet.

The authors are with the Department of Electrical Engineering, University of Toronto, Toronto, Ontario, Canada M5S-1A4.

IEEE Log Number 9104049.

[1]Here, motion detection means the detection of a movement in the image projected onto the imager. No velocity computation is implied [6].

[2]The biological visual system can detect motion of images that are both time variant and spatially variant. To mimic this type of operation requires both integrating and differentiating the output of the photosensor and is a subject for further research.

0018-9200/92$03.00 © 1992 IEEE

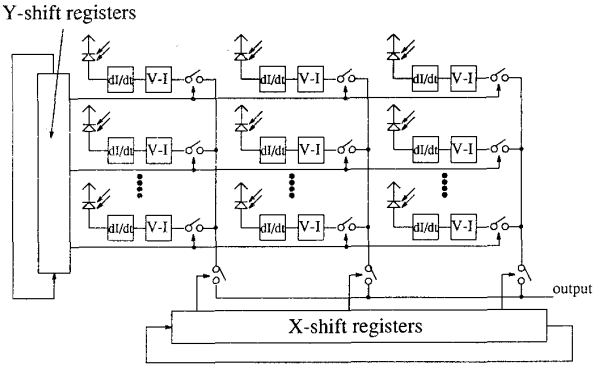

Fig. 1. Architecture of the motion-detecting imager with local sampling.

show how many of the motion-detecting pixels are triggered.

IV. Current-Mirror Differentiator

The difficulty of implementing inductors on VLSI chips makes the direct differentiation of the output current of the photodiode a difficult task. To circumvent this problem, the output current of the photodiode can first be converted to a voltage signal using a logarithmic current-to-voltage converter [7]. A voltage differentiator is then used to differentiate the voltage signal [8]. However, such an approach to temporal differentiation is sensitive to the input offset voltage of the voltage differentiator [2, ch. 10]. This fact is especially important because subthreshold MOSFET's, which have relatively poor matching characteristics [3], [9], are likely to be used for the voltage differentiator to lower the power consumption. Avoiding differential pairs that are sensitive to device mismatches [10] can significantly improve the yield of the silicon implementation. It is also possible to perform discrete-time current differentiation using current copier cells [11]–[13]. However, switching noise limits the usefulness of the current copiers in low-current applications [14]–[16].

A novel current differentiator using a current mirror is shown in Fig. 2. A transconductance amplifier driving an integrating capacitor is added to the feedback loop of the current mirror to convert it into a current differentiator. The input current is injected into node A, and the output voltage is observed at the same node.

Linear analysis shows that if the frequency of the input signal is low enough such that $s << r_{o2} G_{mc} (g_{m1} // g_{m3})/C$, where G_{mc} is the gain of the transconductance amplifier, g_m is the transconductance of the individual transistor, and r_{o2} is the output resistance of transistor n_2, then the output voltage is the first-order time derivative of the input current given by

$$\frac{v_o}{i_{in}} \approx \frac{sC}{G_{mc}(g_{m1} // g_{m3})}. \tag{1}$$

Thus, the current mirror (CM) is operating as a current differentiator, which will be referred to as the CM differentiator.

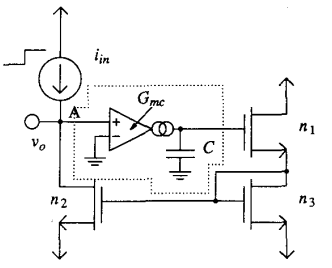

Fig. 2. CM differentiator.

When a step current is injected into node A, the gate voltage of n_1 cannot rise instantly to increase the drain current of n_2 due to the delay in charging C. This leads to a large overshoot of the output voltage. To increase the sensitivity of the CM differentiator in order for it to response to very small input currents, the maximum output driving current of the transconductance amplifier must be as low as possible. This coupled with a large enough input-current step size will overdrive the CM differentiator and cause its output to saturate at its maximum value $v_{o\max}$ as shown in Fig. 3.

The CM differentiator can be characterized in terms of its response time T_R and its normalized output-response voltage O_R. If at t_1 and t_2 ($t_2 > t_1$), the output voltage is $v_{o\max}/\sqrt{2}$, the response time T_R of the CM differentiator can be defined as

$$T_R = t_2 - t_1. \tag{2}$$

If at $t = \infty$, $v_o = v_F$, the normalized output-response voltage O_R of the CM differentiator can be defined as

$$O_R = \frac{v_{o\max} - v_F}{v_{o\max}}. \tag{3}$$

Neglecting the rise time of the output voltage and any second-order effect such as charge pumping, the response time of the CM differentiator can be expressed as

$$T_R = \frac{C}{i_{c\max}(g_{m1} // g_{m3})}\left[i_{in} - \frac{v_{o\max}}{\sqrt{2} r_{o2}}\right] \tag{4}$$

where $i_{c\max}$ is the maximum output current of the transconductance amplifier and i_{in} is the input current. Note that T_R increases with increasing i_{in}. However, as will be shown below, this is only true if charge-pumping effects are negligible. Ideally, the value of O_R should be as close to unity as possible, and the response time should be in the millisecond range.

To achieve analog VLSI density, a very simple transconductance-amplifier configuration must be used. This leads to a large input offset voltage. However, in the present design, the transconductance amplifier is part of the negative-feedback loop that greatly reduces potential current mismatches due to the input offset voltage of the transconductance amplifier. For example, using an input-offset voltage of 1 V and an input current of 10 nA, analysis shows that the mismatch of the drain currents of n_2

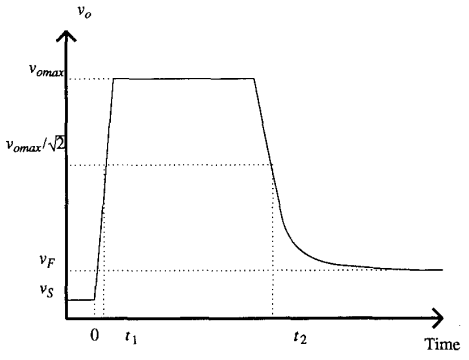

Fig. 3. Output voltage of the overdriven CM differentiator.

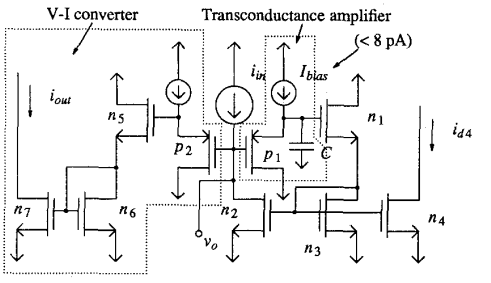

Fig. 4. CM differentiator used in the pixel. Power supply voltages are ±5 V.

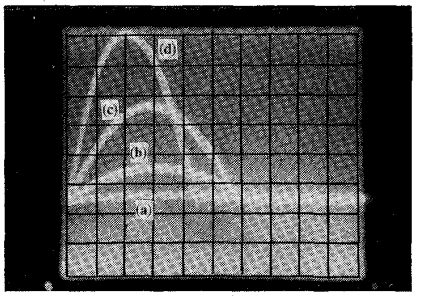

Fig. 5. Output voltage of the CM differentiator. The step sizes of the input current are (curve (*a*)) 20 pA, (curve (*b*)) 45 pA, (curve (*c*)) 106 pA, and (curve (*d*)) 1.2 nA. The vertical scale is 1 V/div and the horizontal scale is 2 ms/div.

and n_3 is less than 10%. Moreover, the input-offset current of the CM differentiator is negligibly low even if a large input-offset voltage transconductance amplifier is used. On a CMOS chip, the simplest available transconductance amplifier is the MOSFET itself. Fig. 4 shows a CM differentiator using a p-MOSFET as the transconductance amplifier. Also shown in Fig. 4 is the voltage-to-current converter required for the implementation of the wired-OR gate for generating the interrupt signal for an external image capturing system.

The sensitivity of the CM differentiator is a function of the dc input current controlling the output impedance of n_2 in Fig. 2. In a noisy environment, the dc input current (produced by an independent current source) must be increased to reduce r_{o2}, and thus the sensitivity of the CM differentiator. As long as the input current is much larger than the noise current, the CM differentiator can be biased in such a way that its response will be dominated by the step input current.

The CM differentiator will not oscillate unless the parasitic capacitance C_{in} at node A is infinitely large. However, to avoid excessive ringing (long settling time), the following condition must be met [17]:

$$C > 4r_{o2}^2 G_{mc}(g_{m1} // g_{m3}) C_{in}. \tag{5}$$

This condition is easily met by the CM differentiator with very small I_{bias}.

V. Experimental Results

The CM differentiator shown in Fig. 4 used in the implementation of the motion-detecting imager was fabricated using a 3-μm CMOS process.

When excited by an input current step ranging from 20 pA to 1.2 nA, the output voltage of the CM differentiator is shown in Fig. 5. Note that the response time is not significantly reduced when the step size of the input current is low. However, when the step size of the input current is increased to over 1 nA, significant reduction of the response time is observed. The reduction in the response time of the CM differentiator when the input step size is large is due to charge-pumping effects. The sine-wave shape of the output voltage indicates the transconductance amplifier is operating in the linear range of operation and its output current does not saturate.

When the input step is small, the rate of increase of the output voltage is low. This gives sufficient time for the channel charge pumped out of p_1 in Fig. 4 to be drained away through the drain of p_1. However, as the input step size increases, the rate of increase of the output voltage grows. This causes p_1 to be switched off in a very short time and most of the channel charge is trapped and pumped into the integrating capacitor C. Thus, the integrating capacitor receives positive charge through charge-pumping and the tail-end biasing current I_{bias}. This leads to shorter response time.

The measured normalized output-response voltage and response time as functions of I_F/I_S and the slew rate of the input current are plotted in Figs. 6 and 7, respectively. The value of I_S, the initial value of a positive step input current, for all cases is 80 pA. I_F is the final value of the input current. The experimental results clearly show that the CM differentiator is capable of differentiating and detecting an input current in the subnanoampere range.

The motion-detecting imager using the architecture shown in Fig. 1 was also implemented using 3-μm CMOS technology. The total number of pixels is 25 by 25. Each pixel occupies an area of 0.022 mm^2 which leads to a pixel density of 45 pixels/mm^2. The pixel density can be increased by using a better layout technique and a simpler voltage-to-current converter. To reduce power supply noise, the pixel array and the shift registers have separate

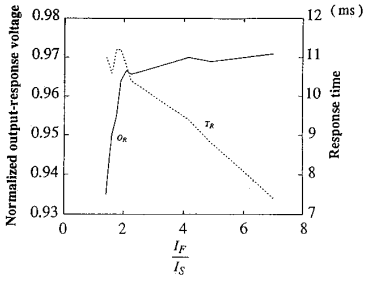

Fig. 6. Measured normalized output-response voltage (O_R) and response time (T_R) as functions of I_F/I_S.

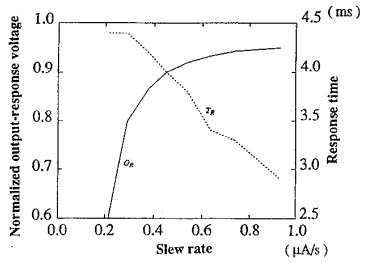

Fig. 7. Measured normalized output-response voltage (O_R) and response time (T_R) as functions of the slew rate of the input current.

supply rails. The imager was tested and was found to be functional. Experimental results of the imager will be reported in the near future [17].

VI. Conclusion

An analog technique for detecting image motion was reported. Based on this technique, a motion-detecting imager using a novel subnanoampere current differentiator was successfully implemented using 3-μm CMOS technology. The pixel density achieved was 45 pixels/mm^2. To achieve higher pixel densities, a more compact current differentiator and smaller photodiodes are required. Future work should focus on reducing the size of the CM differentiator and on the implementation of a complete vision system with motion-detection capability on a single chip.

References

[1] C. Mead and M. Ismail, *Analog VLSI Implementation of Neural Systems*. Boston: Kluwer, 1989.
[2] C. Mead, *Analog VLSI and Neural Systems*. Reading, MA: Addison-Wesley, 1989.
[3] A. G. Andreou, "Current-mode subthreshold MOS circuits for analog VLSI neural systems," *IEEE Trans. Neural Networks*, vol. 2, pp. 205-213, 1991.
[4] C. A. Mead, X. Arreguit, and J. Lazzaro, "Analog VLSI model of binaural hearing," *IEEE Trans. Neural Networks*, vol. 2, pp. 230-236, 1991.
[5] A. Gruss, L. R. Carley, and T. Kanade, "Integrated sensor and range-finding analog signal processor," *IEEE J. Solid-State Circuits*, vol. 26, pp. 184-191, 1991.
[6] C. L. Lee, S. Chang, and C. W. Jen, "Motion detection and motion adaptive pro-scan conversion," in *Proc. IEEE ISCAS*, 1991, pp. 666-669.
[7] C. Mead, "A sensitive electronic photoreceptor," in *Proc. Chapel Hill Conf. VLSI*, 1985, pp. 463-471.
[8] M. A. Sivilotti, M. A. Mahowald, and C. A. Mead, "Real-time visual computations using analog CMOS processing arrays," in *Proc. Stanford Conf. Advanced Research VLSI*, 1987, pp. 295-312.
[9] E. Vittoz and J. Fellrath, "CMOS analog integrated circuits based on weak inversion operation," *IEEE J. Solid-State Circuits*, vol. SC-12, pp. 224-231, 1977.
[10] P. E. Allen and D. R. Holberg, *CMOS Analog Circuit Design*. New York: HRW, 1987.
[11] D. Vallancourt, Y. P. Tsividis, and S. J. Daubert, "Current-copier cells," *Electron. Lett.*, vol. 24, pp. 1560-1562, 1988.
[12] G. Wegmann and E. A. Vittoz, "Very accurate dynamic current mirrors," *Electron. Lett.*, vol. 25, pp. 644-646, 1989.
[13] J. B. Hughes, I. C. Macbeth, and D. M. Pattulo, "Switched-current system cells," in *Proc. IEEE ISCAS*, 1990, pp. 303-306.
[14] H. C. Yang, T. S. Fiez, and D. J. Allstot, "Current feedthrough effects and cancellation techniques in switched-current circuits," in *Proc. IEEE ISCAS*, 1990, pp. 3186-3188.
[15] T. Fiez and D. J. Allstot, "CMOS switched-current ladder filters," *IEEE J. Solid-State Circuits*, vol. 25, pp. 1360-1367, 1990.
[16] S. J. Daubert and D. Vallancourt, "Noise analysis of current copier circuits," in *Proc. IEEE ISCAS*, 1990, pp. 307-310.
[17] C. P. Chong, "Analog VLSI parallel-processing arrays," Ph.D. disertation, Dept. of Electrical Eng., Univ. of Toronto, in preparation.